



## Geomorphic structure of tidal hydrodynamics in salt marsh creeks

Sergio Fagherazzi,<sup>1</sup> Muriel Hannion,<sup>2</sup> and Paolo D'Odorico<sup>3</sup>

Received 21 June 2007; revised 22 November 2007; accepted 3 December 2007; published 13 February 2008.

[1] This paper develops a geomorphological theory of tidal basin response (tidal instantaneous geomorphologic elementary response, or TIGER) to describe specific characteristics of tidal channel hydrodynamics. On the basis of the instantaneous unit hydrograph approach, this framework relates the hydrodynamics of tidal watersheds to the geomorphic structure of salt marshes and, specifically, to the distance traveled by water particles within the channel network and on the marsh surface. The possibility of determining the water fluxes from observations of geomorphic features is an appealing approach to the study of tidally driven flow rates. Our formulation paves the way to the application of recent results on the geomorphic structure of salt marshes and tidal networks to the determination of marsh creek hydrology. A case study shows how the asymmetry in the stage-velocity relation and the existence of velocity surges typical of the tidal hydrographs can be explained as an effect of the delay in the propagation of the tidal signal within the marsh area.

**Citation:** Fagherazzi, S., M. Hannion, and P. D'Odorico (2008), Geomorphic structure of tidal hydrodynamics in salt marsh creeks, *Water Resour. Res.*, 44, W02419, doi:10.1029/2007WR006289.

### 1. Introduction

[2] Salt marshes are important transitional areas between terrestrial and marine environments where exchanges of sediments and nutrients are modulated by tidal oscillations [Fagherazzi *et al.*, 2004]. Most of the water, sediment, and nutrient fluxes between marshes and the ocean take place through systems of low-order networks of tidal creeks, which dissect the salt marsh landscape providing preferential pathways for marsh flooding and drainage during the tidal cycle. Because the transport of sediments and solutes is driven by water flow, the study of water exchange in creek-marsh systems is fundamental to the understanding of the biogeochemistry and sediment budget of tidal basins. Some of the solutes transported by water undergo chemical reactions and are transformed into different chemical compounds during their residence within the marsh-tidal creek system. Thus the study of the biogeochemistry of these environments requires also an assessment of the residence times and their distribution within the tidal basin. The hydrology of tidal basins is typically investigated through rather complex two- or three-dimensional hydrodynamic models, which solve the mass and momentum balance equations in a spatially explicit domain [e.g., Carniello *et al.*, 2005; D'Alpaos and Defina, 2007; Lawrence *et al.*, 2004]. These models provide a detailed representation of the hydrodynamics of the system at the expenses of the com-

plexity associated with numerical algorithms, computational times, and the estimation of a number of parameters. This complexity may prevent the direct assessment of the main geomorphic controls on the hydrologic response of tidal watersheds, particularly in the case of long-term computationally intensive analyses. While in fluvial systems the relation between form and (hydrologic) function has been established by elegant hydrological and geomorphological theories [Gupta *et al.*, 1980; Rodriguez-Iturbe and Valdes, 1979; Rinaldo *et al.*, 1991], the hydrodynamic response of tidal basins has never been explicitly related to the geomorphology of these systems in the context of an analysis of hydrologic transport by travel times [e.g., Woldenburg, 1972; French and Stoddart, 1992; Zeff, 1999].

[3] The lack of a simplified framework for the study of water flow in tidal creeks is a major limitation to the understanding of salt marsh hydrology and biogeochemistry. Because tidal basins are seldom instrumented for stream gauging, the possibility of determining the water fluxes from observations of geomorphic features is an appealing approach to the study of tidally driven flows.

[4] This paper will capitalize on the existing literature on geomorphological theories of the hydrologic response in fluvial networks [Rodriguez-Iturbe and Valdes, 1979; Gupta *et al.*, 1980; Rodriguez-Iturbe and Rinaldo, 1997] to develop a minimalist framework for the study of the response of marsh-tidal creek systems forced by the tidal cycle. This framework will be used to investigate some fundamental features of the basin response, including the geomorphic controls, the ability to infer morphological properties of the marsh-creek system from flow records, and the possible existence of hysteresis in the stage-discharge relation.

[5] Field studies [Myrick and Leopold, 1963; Pethick, 1972; Bayliss-Smith *et al.*, 1978; French and Stoddart, 1992] have reported a general tendency for an hysteresis

<sup>1</sup>Department of Earth Sciences and Center for Computational Science, Boston University, Boston, Massachusetts, USA.

<sup>2</sup>Department of Geological Sciences, Florida State University, Tallahassee, Florida, USA.

<sup>3</sup>Department of Environmental Sciences, University of Virginia, Charlottesville, Virginia, USA.

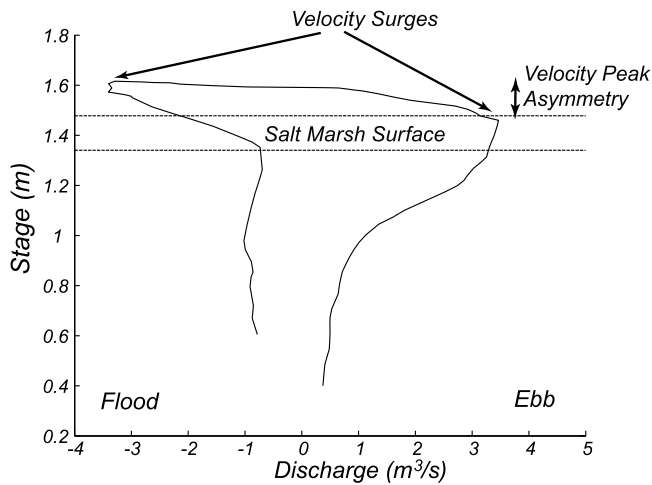


**Figure 1.** Stage-discharge relationship for a tidal marsh creek in Warham, UK. Data are derived from *Bayliss-Smith et al.* [1978], *Pethick* [1980], and *Healey et al.* [1981].

in the stage-discharge (or velocity) relation in salt marsh channels; that is, for a same stage value the discharge can be different in magnitude during the ebb and flood phases of the tidal cycle.

[6] All these studies point out two important characteristics of tidal flow in salt marshes: (1) Tidal velocities show a characteristic series of surges during flood and ebb; the velocity is low when the water is confined in the channel during a tidal cycle, but it largely increases, producing a surge, when the marsh platform is inundated; and (2) the velocity surge is asymmetric between flood and ebb; the velocity peak during flood occurs for water levels above the marsh surface, whereas during ebb the velocity peaks when the water is below the marsh surface (Figure 1).

[7] *Boon* [1975] proposed a simple model based on the continuity equation to simulate the formation of velocity surges in salt marsh channels and compared his results with records of tidal discharge taken at the inlet of a salt marsh drainage system near Wachapreague, Virginia. *Boon's* [1975] model expresses the discharge  $Q$  through the channel mouth as

$$Q = S \frac{dh}{dt}, \quad (1)$$

where  $h$  is the stage,  $dh/dt$  is rate of change in tidal elevation, and  $S$  is the inundated surface at stage  $h$ . The model assumes that the channel is frictionless, the water surface is horizontal, all the water enters or leaves the marsh drainage basin through the channel, and both wind stress and the effect of inertial forces are negligible (i.e., the celerity of the tidal wave is infinite). Under these assumptions the right-hand side of (1) simply represents the tidal prism entering or leaving the channel cross section. Therefore, in this model [*Boon*, 1975], the drainage basin morphology, expressed through the hypsometric curve  $S(h)$  determines the velocity surges. The results of this simple tidal model match, in first approximation, the discharges measured in the tidal creek.

[8] Equation (1) provides a simple and elegant explanation for velocity surges in salt marsh creeks: The discharge

increases during overbank flow, because more water has to be conveyed in the channel to cover a larger area when the marsh is inundated during flood. Similarly, during ebb, a drop in tidal elevation conveys more water out of the channel when the marshes are inundated because a larger area needs to be drained. Nevertheless, equation (1) is unable to capture the asymmetry of the velocity surges, since they both occur when the right-hand side of (1) reaches its maximum value, i.e., when the tidal elevation is just above the marsh platform level.

[9] To improve this model, *Pethick* [1980] included in the formulation an asymmetric tide and a network of channels that branch out in the salt marsh. Model simulations show that shallow-water asymmetric tides are responsible for velocity asymmetry, whereas the branching of the channel network determines the position and strength of the velocity surges.

[10] *Healey et al.* [1981] challenged these two models on the basis of field data showing that the asymmetry of the time-stage curve does not occur for all tides and that the water surface does not remain horizontal during the flood and ebb cycles. However, the slope of the water surface in intertidal basins whose dimensions are much smaller than the tide wavelength has only a second-order effect on the continuity equation [*Fagherazzi*, 2002; *Fagherazzi et al.*, 2003]. Thus equation (1) still captures the basic characteristics of the system.

[11] This paper develops a geomorphological theory of tidal basin response that overcomes the limitations of previous approaches [*Boon*, 1975]. The asymmetry in flow hydrodynamics will be explained as an effect of the delay in the propagation of the tidal signal within the marsh area.

## 2. The Tidal Instantaneous Geomorphologic Elementary Response Model

[12] The main limitation of the continuity model presented by *Boon* [1975] is the implicit assumption that the tide propagates instantaneously across the marsh system.

[13] As a result, in *Boon's* [1975] model an increase or decrease in tidal elevation leads to an instantaneous increase or decrease in the tidal flow at the channel mouth, since  $Q$  increases with  $dh/dt$  (equation (1)). Thus during flood all the water particles entering the marsh system from the creek move instantaneously to the marsh (provided that  $h$  exceeds the marsh elevation), thereby increasing the water level across the marsh to perfectly match the tidal level. Similarly, during ebb, all the particles move instantaneously from the marsh platform to the channel mouth to adjust without delay to the decreasing tidal level. A more realistic approach would account for the travel time of each water particle from the channel mouth to every location within the marsh platform. In fact, during flood the peak velocity in the creek is delayed with respect to the flooding of the marsh platform, since it takes a finite period of time for the creek to be affected by the flooding of the marsh surface. Similarly, during ebb, the discharge peak is delayed with respect to the drainage of the marsh surface, due to the finite period of time the water particles take to move from each point of the flooded surface of the marsh to the mouth of the tidal creek.

[14] In this study we draw on the geomorphologic theory of the hydrologic response for fluvial systems to relate the

distribution of travel times to the asymmetry of tidal flow in salt marsh creeks. The distribution of travel times will be then computed from the geomorphic structure of the tidal marsh. To this end, we will focus on ebb and flood conditions separately.

### 2.1. Ebb Flow From the Marshes to the Tidal Creeks

[15] We first consider the case of ebb flow and assume that the system is initially at a steady state, i.e., the marshes are partly flooded and the water surface is horizontal with elevation  $h_0$ . At time  $t = 0$  the water level in the creek at the outlet  $O$  of the tidal basin drops by  $dh$  (i.e., from  $h_0$  to  $h_0 - dh$ ) and water starts flowing from the marshes into the nearby creeks, and then through the creek network toward  $O$ . Different parts of the tidal basin contribute to the flow at the outlet  $O$  at different times depending on their “hydraulic distance” from  $O$ . This situation is similar to the case of water transport in a river basin receiving an effective precipitation  $dh$  uniformly distributed across the basin, in that all rain water reaching the basin collects in the channel network and is delivered to only one outlet point.

[16] The relation existing in river basins between the hydrograph,  $Q(t)$ , measured at the outlet and uniform rainfall inputs has been often investigated using the linear theory of the hydrologic response. This theory postulates that it is possible to express the hydrograph generated by a given rainstorm as the sum of the basin responses to a sequence of rainfall inputs occurring in the course of the rainstorm. This framework has led to the theory of the unit hydrograph [Sherman, 1932], which expresses the storm-flow hydrograph as a function of storm hyetograph and basin properties, with the latter being expressed by a response function, known as unit hydrograph (UH). In this study we will refer to the concept of instantaneous UH (IUH), defined as the direct runoff hydrograph resulting from an instantaneous rainfall excess uniformly distributed over the drainage area [e.g., Chow *et al.*, 1988]. The IUH theory invokes the linearity of the system to express the response to a rainfall pulse  $dP$  as  $dQ(t) = dP IUH(t)$ . If we assume that the IUH is an invariant property of the basin (i.e., the function  $IUH(t)$  does not change in the course of the event nor from event to event), the response to an effective storm hyetograph,  $I(t)$ , can be expressed as the integral sum of the pulse responses  $dQ(t)$

$$Q(t) = \int_0^t I(\tau) IUH(t - \tau) d\tau, \quad (2)$$

where  $I(t)$  represents the rainfall intensity,  $I(t) = dP(t)/dt$ , with  $P$  being the rainfall depth.

[17] The basin-specific response function  $IUH(t)$  has been related to the geomorphic structure of the watershed [Rodriguez-Iturbe and Valdes, 1979] and interpreted as the by-product of the basin area times the probability density function  $f(t)$  of travel times from any point in the basin to the outlet [Gupta *et al.*, 1980]. The travel time distribution can be directly related to the geomorphic characteristic of the watershed (section 2.3).

[18] The application of this framework to ebb flow in tidal basins is relatively straightforward. In this case a decrease  $dh$  in water depth at the outlet corresponds to a

depth  $dh$  of water excess across the flooded part of the marsh. Thus in equation (2) the storm hyetograph  $I(t)$  can be simply replaced by the rate  $dh/dt$  of tidal stage decrease at the outlet; that is, the hyetograph is substituted with the volumetric input of water driven by tidal oscillations (equation (1)). Moreover, in this case the impulse response function  $IUH$  is again the product of the basin area  $S$  times the travel time distribution  $f(t)$  of a unit amount of water particles (uniformly distributed in space) instantaneously leaving the watershed. A major difference with respect to river basins is that in creek-marsh systems subjected to tidal fluctuations both the contributing area  $S$  and the distribution of residence times depend on the spatial extent of the flooded marshes, which, in turn, depends on the stage  $h$  (and time, if propagation effects are accounted for). Thus the convolution integral in (2) becomes

$$Q = \int_0^t S(h) \frac{dh}{dt} f_h(t - \tau) d\tau, \quad (3)$$

where  $S(h)$  is the hypsometric curve and  $f_h(t)$  is the state-dependent travel time distribution. Because of this state-dependence, this IUH is in general noninvariant. Section 3 will discuss the dependence of  $f_h(t)$  on the geomorphic features of the tidal basin and present suitable methods for its calculation.

[19] The proposed framework is based on a few simplifying assumptions: (1) The distributions of travel times from each marsh site are assumed to be independent, despite their dependence on the spatially correlated water surface. Similar assumptions were used in the application of the transport theory by travel times to river basins; (2) the IUH will be expressed as a function of the state of the system only through the hypsometric curve, which provides the flooded area as a function of stage. However, the dependence of the flow velocity on the water depth over the marsh and on its spatial gradients will not be accounted for. This effect would further contribute to the state dependence of the probability distribution of travel times; (3) the probability distribution of travel time will be calculated assuming that for any given stage  $h$ , all points in the flooded area,  $S(h)$ , are hydraulically connected to the outlet (i.e., with no isolated areas).

### 2.2. Flood of the Salt Marshes

[20] During the flood phase of the tidal cycle any increment  $dh$  in stage at the inlet  $O$  is associated with a water flow into the tidal watershed, and with the consequent flooding of the marshes (i.e., increase in water depth and extent of flooded area). The relation between  $dh$  and the rate of flow through the inlet depends on the hypsometry and the planar geometry of the creek-marsh landscape.

[21] We assume that the system is linear and that the hydrograph generated by increasing water levels at the inlet can be expressed as a convolution integral of the responses to pulse increments  $dh$ , similarly to the approach described in the previous section for ebb flow conditions (equation (2)). In this case the instantaneous response function  $IUH$  is defined as the hydrograph generated at the inlet by a unit increment in stage with the water surface being initially

horizontal across the flooded portion in the watershed. It can be shown that even in this case the  $IUH(t)$  can be expressed as the by-product of the flooded area,  $S(h)$ , by the probability distribution of travel times of water particles moving from the inlet to all points of the watersheds that have been reached by the wetting front. This fact can be shown following an approach similar to the proof developed by *Gupta et al.* [1980]. In fact, at any time  $t$  the continuity equation for the watershed can be expressed as

$$\frac{dVol(t)}{dt} = Q_{in}(t) - Q_{out}(t), \quad (4)$$

where  $Vol$  is the water volume stored in the watershed, while  $Q_{in}$  and  $Q_{out}$  are the inflow and outflow rates through the boundaries of the watershed. In the course of the flood phase of the tidal oscillation we have that  $Q_{out} = 0$ . An instantaneous increase at time  $t_0 = 0$  in the water level at the inlet from  $h_0$  to  $h_0 + dh$  is associated with a storage volume,  $Vol(t) = dh \eta_t(h)S(h)$ , with  $\eta_t(h)$  being the fraction of the area  $S(h)$  that has been reached at time  $t$  by water particles entering the inlet at time  $t_0$ . We follow *Gupta et al.* [1980] and express  $\eta_t(h)$  using a discrete representation of the watershed as a finite set of sites  $i$ . We also assume that the flooding of any site  $i$  is independent of the state of the other sites existing within the watershed. Thus, if  $T_i$  is the (random) travel time of a water particle moving from the inlet to site  $i$ , the times  $T_i$  ( $i = 1, 2, \dots, n$ ) can be assumed to be a set of independent and identically distributed random variables, with  $n$  being the number of sites existing within the area  $S(h)$ . The fraction  $\eta_t(h)$  of the flooded area reached by the tidal wave at time  $t$  is then proportional to the number of sites  $i$  having travel time  $T_i \leq t$ , i.e., to the probability  $P_h[T_i \leq t]$  that  $T_i \leq t$ . Thus the storage volume is

$$Vol_h(t) = dhS(h)P_h[T_i \leq t], \quad (5)$$

where the subscript  $h$  stresses the fact that the fraction of flooded area is calculated with respect to the "wetable area"  $S(h)$ , when the stage is  $h$ .  $S(h)$  depends on the geomorphic features of the catchments and is usually expressed by the hypsometric curve. The instantaneous unit response function for flood conditions can be determined using equations (4) and (5) with  $dh = 1$  (unit increase in water level),  $Q_{out} = 0$ , and neglecting changes in the spatial extent of the wetted areas (i.e., in  $S(h)$  and  $n$ ),

$$IUH = S(h)f_h(t), \quad (6)$$

with  $f_h(t)$  representing the probability density function of travel times when the stage is  $h$ . Equation (6) indicates that the hydrologic response of a tidal basin can be expressed with (3) as a function of the travel time distribution both in the case of ebb and of flood flow.

### 2.3. Travel Time Distribution

[22] Sections 2.1 and 2.2 indicate that both flood and ebb flows depend on the travel time distribution,  $f_h(t)$ . In what follows we will investigate the properties of  $f_h(t)$  and relate them to the geomorphic features of the tidal basin. To this end, we assume that  $f_h(t)$  depends only on the stage  $h$  and not also on the flow direction (i.e., ebb or

flood flow). In other words, we postulate that both the travel velocities and the travel distances,  $x_i$ , between any point  $i$  in the watershed and the inlet/outlet  $O$  are independent of the flow direction. However, because wetting and drying processes may proceed at different velocities, this framework can be easily generalized using in the calculation of  $f_h(t)$  (equations (7) and (9)) different velocity values during flood and ebb. As noted, we will also assume that the propagation of water particles along the drainage/flood path,  $\gamma_i$ , connecting  $i$  to  $O$  is independent of the flow conditions along other paths, and that the hydraulic distance  $x_i$  is the only geomorphic attribute of  $\gamma_i$  affecting the distribution of the travel time  $T_i$  associated with the path  $\gamma_i$ . Thus the distribution of travel times for the whole basin can be calculated as the travel time distribution  $f(t|x)$  for paths of length  $x$ , integrated over the whole distribution of the path lengths existing within the basin

$$f_h(t) = \int_0^L W_h(x)f(t|x)dx, \quad (7)$$

where  $L$  is the length of the longest path, while  $W_h(x)$  is the path length distribution calculated considering all sites existing within the area  $S(h)$ . Known as "geomorphologic width function" [Shreve, 1969; Kirkby, 1986],  $W_h(x)$  is an empirical function synthesizing the major geomorphic controls on the flooding and drainage of the marsh-creek system. Notice how the subscript  $h$  denotes the dependence of the width function on the stage.

[23] In what follows we will discuss two models for the travel time distribution  $f(t|x)$  conditional on the path length  $x$ . The simplest model of hydrologic transport along a pathway of length  $x$  assumes that the travel velocity  $V$  is constant along the path and that the travel time is a deterministic variable,  $t = x/V$ . In this case the distribution of travel times along the path of length  $x$  is

$$f(t|x) = \delta\left(t - \frac{x}{V}\right), \quad (8)$$

with  $\delta(\cdot)$  being the Dirac's delta function.

[24] Alternatively, we can assume that because of the randomness inherent to the processes of water transport, travel times are random variables associated with a continuous random walk. The resulting stochastic dynamics can be modeled as a Wiener's diffusion process [e.g., *Cox and Miller*, 1965] superimposed to the mean flow, consistently with the parabolic (or diffusive) wave models of de Saint-Venant equations [Rodriguez-Iturbe and Rinaldo, 1997]. The distribution of travel times along a hydraulic path of length  $x$  can be determined as solution of a backward Kolmogorov problem [e.g., *Cox and Miller*, 1965] associated with the Fokker-Plank equation with suitable boundary conditions [Mesa and Mifflin, 1986],

$$f(t|x) = \frac{x}{\sqrt{4\pi Dt^3}} \exp\left[-\frac{(x - Vt)^2}{4Dt}\right], \quad (9)$$

with  $D$  being the coefficient of hydrodynamic dispersion.

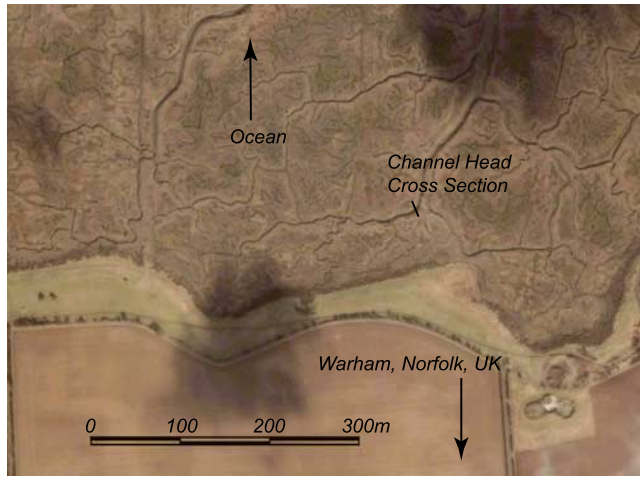


**Figure 2.** Location of the creek cross section studied by *Bayliss-Smith et al.* [1978], *Pethick* [1979], and *Healey et al.* [1981] (courtesy GoogleEarth).

Thus this framework recognizes that the hydrologic transport is determined both by advection and hydrodynamic dispersion.

#### 2.4. Effect of Heterogeneity in the Velocity Field

[25] Equations (8)–(9) assume that water moves between the outlet/inlet  $O$  and any point  $i$  within the basin in a uniform flow with a spatially homogeneous average velocity. This assumption is quite unrealistic, particularly when we observe that part of this path is along the tidal creek network (i.e., with faster and deeper flow), while the remaining part of the path is over the inundated marshes (i.e., with slower and shallower flow). Moreover on the marsh surface the flow velocity is further reduced by vegetation drag [*Temmerman et al.*, 2005a]. We notice that the separation in the velocity scale existing between creeks and marshes resembles the difference observed between hillslopes and channels in river basins. Thus we follow *van der Tak and Bras* [1990] and *D’Odorico and Rigon* [2003], and use two separate velocities,  $V_{marsh}$  and  $V_{channel}$ , for the marsh and creek portion of the hydraulic path, respectively.

[26] If  $t_{marsh}$  and  $t_{channel}$  are the travel times through the marsh and creek, and  $x_{marsh}$  and  $x_{channel}$  are the corresponding “hydraulic lengths,” the travel time between  $i$  and  $O$  is  $t = t_{marsh} + t_{channel}$ , while the “hydraulic distance” is  $x = x_{marsh} + x_{channel}$ . The probability distributions,  $f_{marsh}(t_{marsh}|x_{marsh})$  and  $f_{channel}(t_{channel}|x_{channel})$ , of  $t_{marsh}$  and  $t_{channel}$  can be still calculated either with equation (8) or (9), provided that the velocity  $V$  is replaced with the corresponding velocity,  $V_{marsh}$  or  $V_{channel}$ , and that the dispersion coefficient  $D$  assumes the values  $D_{marsh}$  or  $D_{channel}$ , corresponding to marsh and creek flow, respectively.

[27] A simplified approach accounting for the different velocities in the creek and marsh portion of the flow path is based on the use in equation (7) of the rescaled width function  $W_h(x')$ , defined using rescaled travel distances  $x' = x_{channel} + r x_{marsh}$ , with  $r = V_{channel}/V_{marsh}$  [*D’Odorico and Rigon*, 2003]. In this case the travel time distributions  $f(t|x')$  are calculated assuming that the whole rescaled

distance  $x'$  is traveled at the same velocity,  $V_{channel}$ , and the kinematic-wave model of water transport within a hydraulic path can be calculated using the residence times expressed as

$$t = \frac{x'}{V_{channel}}. \quad (10)$$

[28] Unlike the case of fluvial watersheds where the flow path follows the topographic steepest gradient, in salt marshes the water flows along gradients of water surface. The flow path on the marsh surface can then be computed following the methodology outlined by *Rinaldo et al.* [1999b]. For a salt marsh of small dimensions the water surface at each instant of the tidal cycle can be approximated with a Poisson equation:

$$\nabla_{\eta}^2 = \frac{\Lambda}{z_0^2} \frac{\partial \eta_0}{\partial t}, \quad (11)$$

where  $\eta$  is the elevation of the water surface above or below the average water elevation within the salt marsh,  $\Lambda$  is a friction coefficient,  $\eta_0$  is the tidal elevation at the inlet, and  $z_0$  is the average water depth on the marsh surface. Furthermore, if we assume that the propagation of the tide within the channel network is instantaneous with respect to the propagation on the marsh surface, we can solve equation (11) only for the unchannelized salt marsh area assuming as a boundary condition a constant elevation equal to  $\eta_0$  in the channels and bordering ocean and a no-flux condition at the boundary between salt marsh and mainland. During ebb the flow direction can be then computed along the surface  $\eta$  following the steepest descent gradient until a tidal channel is reached. Once the particle is in the channel, it will travel along the channel network until the channel mouth. Similarly, during flood the particle will first move along the channel network and then proceed along the marsh platform following the same path utilized during ebb, since equation (11) yields identical results for increasing or decreasing water elevations.

### 3. A Case Study

[29] Our model is tested with published data for a tidal creek in the upper marsh at Warham and Stiffkey, North Norfolk, England (Figure 2) [*Bayliss-Smith et al.*, 1978; *Pethick*, 1980; *Healey et al.*, 1981]. The Warham marshes are part of a continuous system which extends along 35 km of coast, from Holme to the west to Cley to the east. The marshes are of the open coast type, partially protected by extensive intertidal sand flats, spits, and barrier islands, and unaffected by freshwater drainage from the land [*Bayliss-Smith et al.*, 1978].

[30] The upper and lower marshes are separated from each other and from the outer flats by transverse creeks. The lower marsh at Warham is drained by a dense network of channels and is vegetated largely with *Aster tripolium* and *Salicornia*. The upper marsh exhibits a stable drainage pattern characteristic of established marsh areas. The marsh is drained by fourth-order creek systems, the main channel being over 20 m wide and 2 m deep [*Bayliss-Smith et al.*, 1978]. In the headwaters, the creeks are mainly 0.5–1.5 m

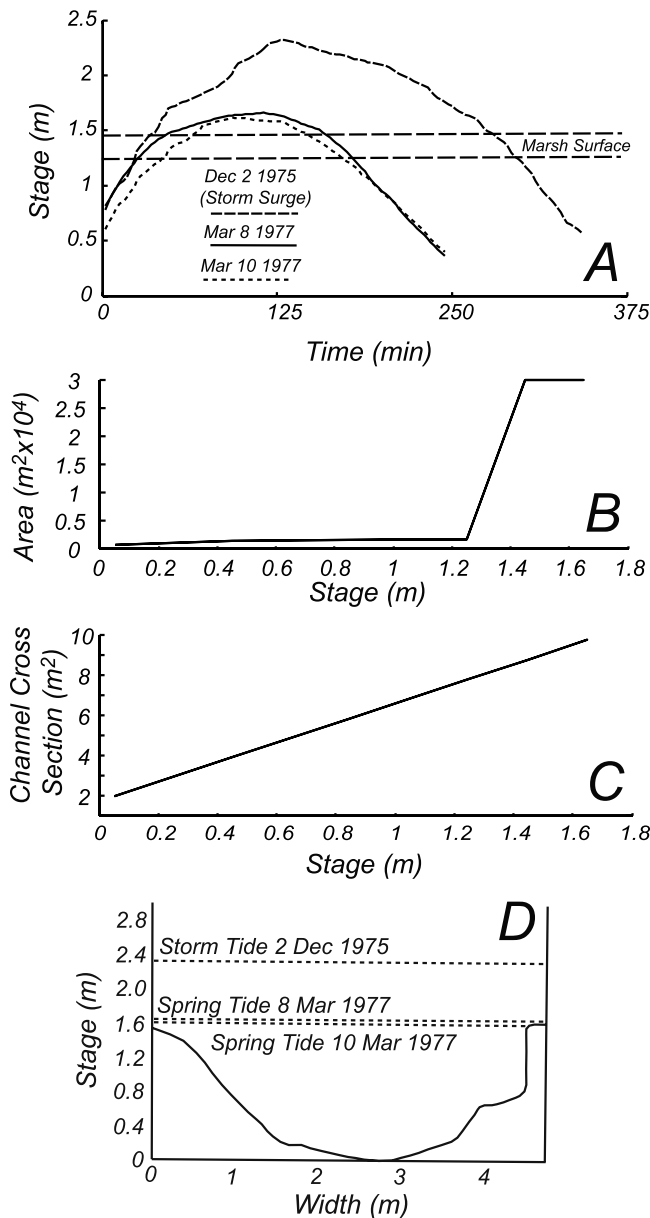


**Figure 3.** Morphological and tidal characteristics of the study site. (a) Tidal stage as a function of time for the tides of 2 December 1975 (storm surge), 8 March 1977, and 10 March 1977 (adapted from *Healey et al.* [1981]). (b) Hypsometric curve of the studied marsh [after *Pethick*, 1980]. (c) Channel cross-sectional area as a function of tidal stage [after *Pethick*, 1980]. (d) Creek cross section [adapted from *Bayliss-Smith et al.*, 1978].

deep. Mean tidal ranges on the Norfolk coast are 2–3 m for neap tides and 5–6 m for spring tide; the area is vulnerable to storm surges.

[31] The velocity and stage data for three tidal surges (2 December 1975, 8 March 1977, and 10 March 1977) were derived from the measurements of *Bayliss-Smith et al.* [1978] and *Healey et al.* [1981] (Figure 3a). The cumulative distribution of area,  $S$ , as a function of tidal elevation (hypsometric curve) and the cross-section area of the

channel,  $A$ , as a function of tidal elevation are reported by *Pethick* [1980] and *Bayliss-Smith et al.* [1978] (Figures 3b, 3c, and 3d); all the data are converted to the reference elevation (ordnance datum) utilized by *Bayliss-Smith et al.* [1978].

[32] We utilize the watershed relative to the channel cross section indicated in Figure 2 and the distribution of channels reported by *Pethick* [1980] (Figure 4a). We then compute the distance of each channel location from the cross section along the channel network (Figure 4b; see also *Fagherazzi et al.* [1999]). The water path on the marsh surface is instead computed following the steepest descent along the water surface (Figure 4c; see also *Rinaldo et al.* [1999a]). Finally, in Figure 4d we report the distribution of the total hydraulic distance (channel distance  $x_c$  plus the distance within the marsh,  $x_m$ ) between the outlet and every point within the marsh watershed. This distribution is shown as a percentage of drainage area in Figure 5a. To calculate the distribution of travel times of water particles during the flooding and drainage of the marsh platform, we need to specify a characteristic water speed in the channel and marsh portion of these paths and then compute the travel times using equation (10).

[33] In Figure 5b we indicate possible distributions of travel times for a channel velocity of 0.5 m/s and different values of water velocity on the marsh ranging from 0.01 to 0.5 m/s. The velocities in both the channel and on the marsh surface are in good agreement with field measurements in marsh systems summarized by *Rinaldo et al.* [1999b]. These distributions of travel times determine the function  $f_h$  in equation (3) and will be used to calculate the tidal discharge and its temporal variability.

#### 4. Results

[34] In a first set of simulations we compare the continuity model (equation (1)) with the tidal instantaneous geomorphologic elementary response model (TIGER) model (equation (3)). We use a simple sinusoidal tide having a period of 12 hours and a total excursion of 5 m, and mean sea level is set at  $-0.85$  m. The calculation proceeds as follow: The tidal elevation  $h$  and the rate of elevation change  $dh/dt$  are computed from the tidal stage hydrograph. The surface  $S$  below water in equation (1) and (3) is determined from the hypsometric curve reported by *Pethick* [1980] (Figure 3b). The distribution of travel times is then determined from equation (10) assuming two values for the velocity for water flow in the channels and on the marsh platforms. The discharge is computed with the convolution reported in equation (3).

[35] The results of the continuity model (equation (1)) of *Boon* [1975] are reported in Figure 6a. As expected, the continuity model captures the two velocity surges when the marsh platform is flooded and drained. At these two instants of the tidal cycle the entire marsh surface is below water ( $S$  is maximum in equation (1)) and the rate of tidal elevation change is the highest within the period of marsh submergence (the rate of tidal elevation change is maximum at mean sea level and decreases to zero at high water). The stage-discharge relationship is symmetrical, since both flood and ebb surges occur at the same tidal elevation. Conversely, the stage discharge relationship of the TIGER model displays the characteristic asymmetry (Figure 6b), with a flood

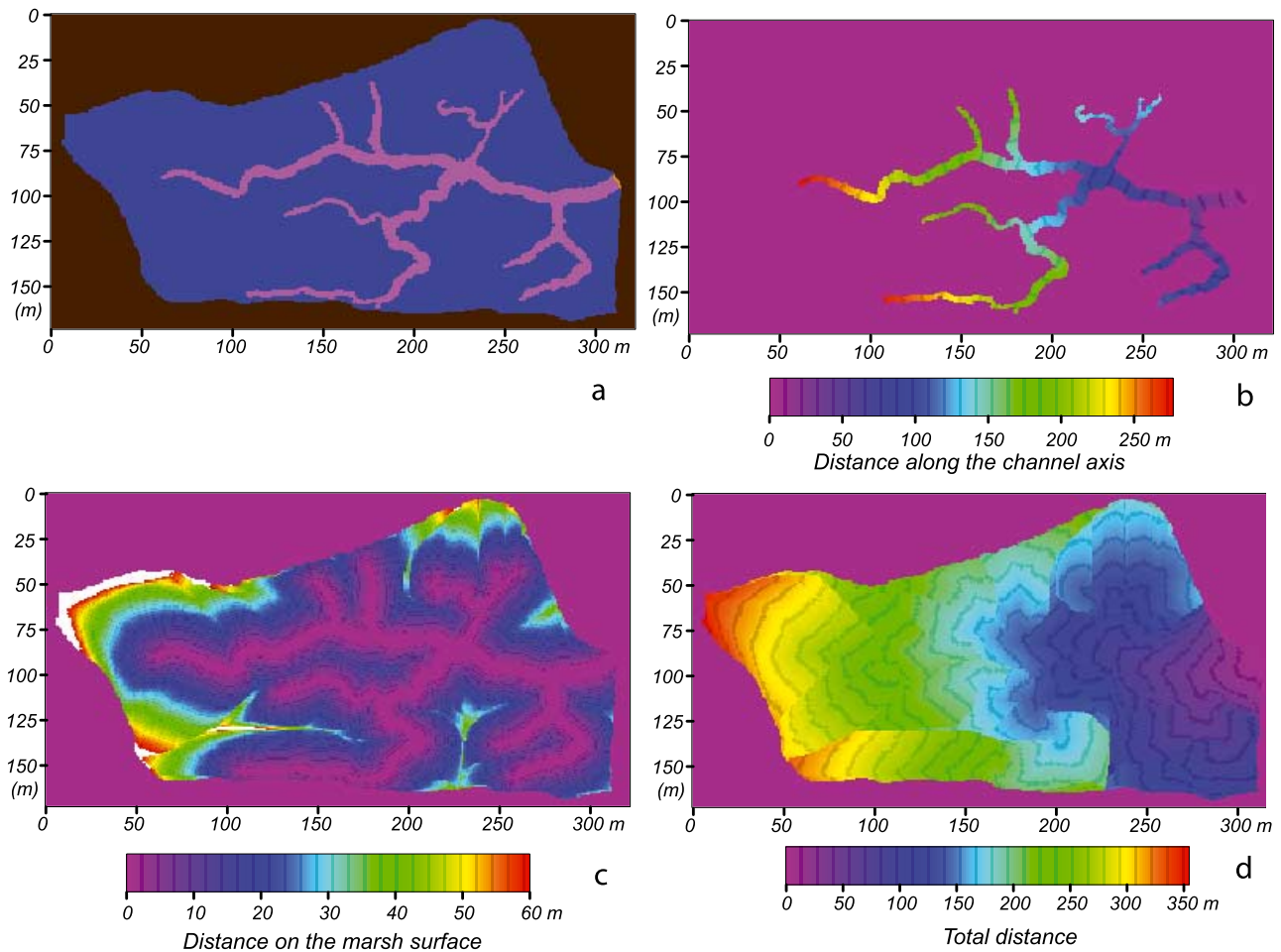


**Figure 4.** Calculation of the hydraulic distances (from the outlet/inlet) in the marsh watershed. (a) Salt marsh watershed and channel network extracted from aerial images. (b) Distances along the channel network. (c) Distances on the marsh surface. (d) Total distance (sum of the distance along the tidal channel and the distance on the marsh platform) for every marsh location.

discharge peak occurring when the water surface elevation is above the marsh surface and an ebb discharge peak for elevations below the marsh surface. The asymmetry increases as the travel times increase. Thus both the distribution of hydraulic distances within the marsh drainage area and the characteristic water velocities can influence the stage-discharge relationship at the channel mouth. Moreover, the convolution in equation (3) reduces the discharge surge when the average travel time on the marsh surface increases. We can then expect that larger salt marshes or salt marshes with a lower drainage density have tidal surges of reduced dimension relative to the drainage area. In fact, in both situations the average travel time is higher, smoothing the discharge peak through the convolution of equation (3).

[36] The flow asymmetry is further enhanced if we consider the relationship between stage and average cross-sectional velocity,  $U$ . In fact, the velocity increases for flows confined within the channel, since for the same discharge the cross-sectional area  $A$  available is less (Figure 3b). Thus, for a sinusoidal tide the stage-velocity relationship displays high velocities during ebb (ebb dominant), when flow is concentrated in the channel.

[37] We then compare the results of the TIGER model with the velocity measurements of *Bayliss-Smith et al.*

[1978] and *Healey et al.* [1981]. In Figure 7a we compare the stage-discharge relationship measured in the field with the one calculated with the continuity model for the spring tide of 8 March 1977. We convert the velocity measurements of *Healey et al.* [1981] in discharge by a multiplication with the creek cross-sectional area reported by *Pethick* [1980] (Figure 3c). As expected, both flood and ebb surges are delayed with respect to the continuity model, even though the magnitude of the discharge peak is of the same order. The delay in discharge peaks is even more obvious if we plot the measured discharge as a function of time versus the discharge obtained from the continuity model (Figures 7b and 7c).

[38] We then account for the delay associated with the distribution of travel times and calculate the discharge hydrograph with the convolution indicated in equation (3). We utilize different values of channel and marsh platform velocity as reported in Figure 5b. The results (Figure 7b) show that the distribution of travel times obtained with a channel velocity of 0.5 m/s and a marsh platform velocity of 0.05 m/s leads to peaks in tidal discharge during flood and ebb that are close to the measured values. However, the phasing is not well captured, with the calculated flood peak occurring before the measured one. Conversely, a marsh

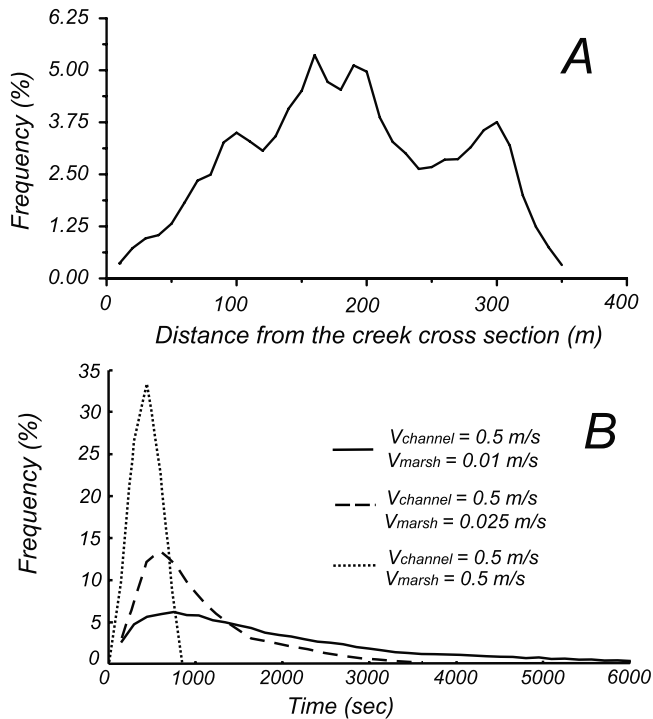


**Figure 5.** (a) Distribution of distances within the marsh watershed from the reference cross section (outlet/inlet). (b) Distribution of travel time for different values of velocities in the channels  $V_{channels}$  and on the marsh surface  $V_{marsh}$ .

platform velocity of 0.025 m/s (Figure 7c) leads to a peak discharge that occurs during flood at the same time as the measured value, but produces an attenuated velocity surge during ebb. An average value of flow velocity between 0.05 and 0.025 m/s can be then considered optimal for the TIGER model. We also note that the model results are very sensitive with respect to the velocity on the marsh surface,

which regulates the distribution of travel times. Finally, the presence of tidal channels increases the propagation speed of the tidal signal, thus reducing the average travel time of water particles (several locations within the marsh can be reached by apical flow from the channel head). As a result the peak discharge increases and the stage-discharge asymmetry is reduced.

[39] We can also attempt to compute the distribution of travel time by deconvolving the measured discharge hydrograph from the discharge calculated from the continuity model (equation (1)). The deconvolution is implemented as follows: First, we subtract the average from the measured discharge hydrograph because for continuity the total volume entering the marsh during flood has to be equal to the total volume exiting the marsh during ebb. Differences between the two volumes can be ascribed to errors in the measurement of the discharge and therefore can be removed. Then we rescale the discharge of the continuity model (equation (3)) so that the tidal prism is identical to the one measured. We note that for the two spring tides of 8 and 10 March 1977 we have to increase the discharge of the continuity model by 30% in order to match the measured tidal prism. This suggests that the total marsh drainage area computed by *Pethick* [1980] might be underestimated. For the storm surge of 2 December 1975 the measured tidal prism instead agrees with the one calculated from the continuity model. To remove finite size effects, we zeropad the discharge for a length 3 times the original signal and we taper the extremities with a second-order polynomial. The result of the deconvolution for the tide of 8 March 1977 is reported in Figure 8a. From this signal we extract the positive component until the first intersection with the  $x$ -axis, in that negative values of  $f(t)$  do not have physical basis. The distribution thus obtained is reported in Figure 8b. In Figure 8c we compare the results of the TIGER model based on the two distributions reported in Figures 8a and 8b with the measured discharge. Both distributions of travel times lead to a discharge hydrograph that well matches the

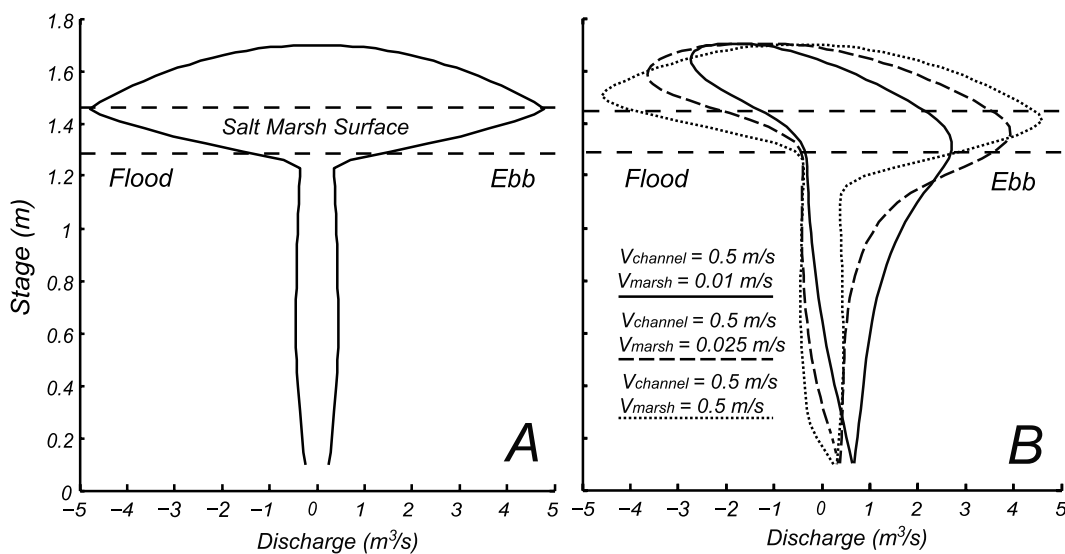


**Figure 6.** Stage-discharge relationships for a sinusoidal tide of maximum amplitude of 2.5 m in the marsh system indicated in Figure 3. (a) Continuity model of *Boon* [1975]. (b) Tidal geomorphic unit hydrograph model with different values of the velocities in the channels  $V_{channels}$  and on the marsh surface  $V_{marsh}$ .



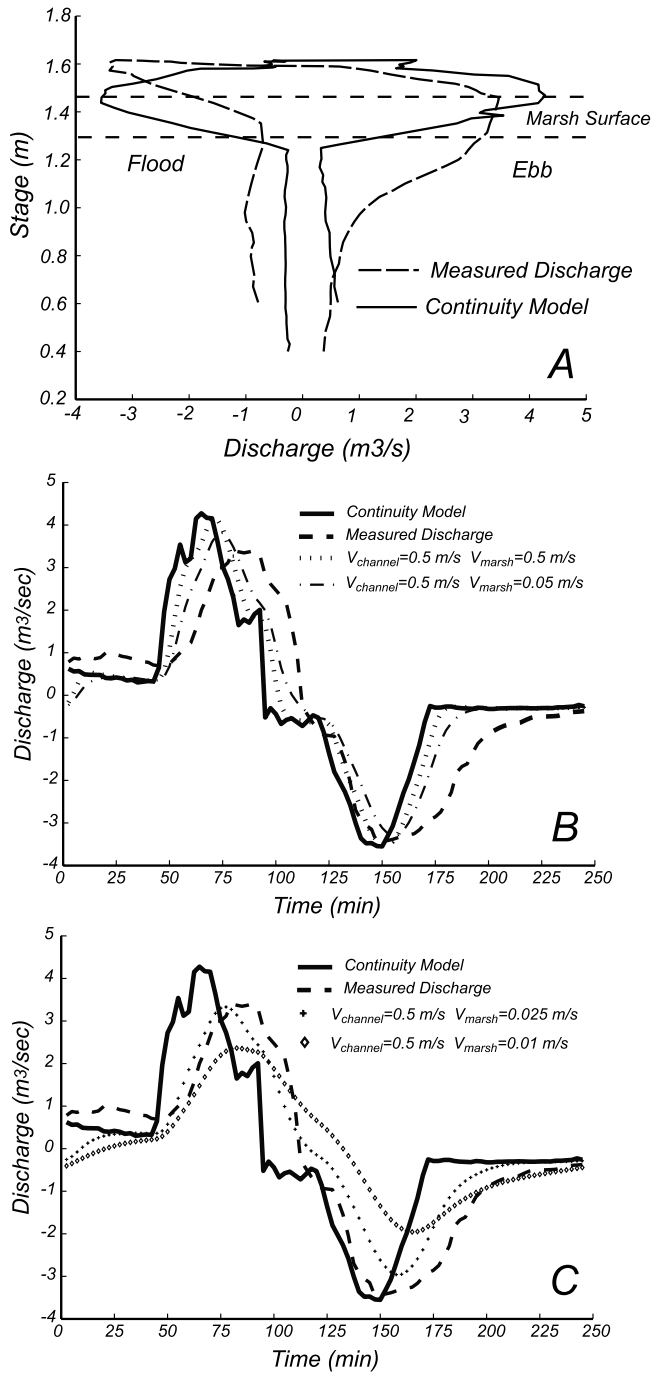


**Figure 7.** Comparison between computed and measured discharges for the tide of 8 March 1977. (a) Comparison between the measured discharges and the continuity model of Boon [1975]. (b and c) Comparison among measured discharges in time and the results of the continuity model and the tidal instantaneous geomorphologic elementary response model (TIGER) model with different values of the velocities in the channels  $V_{channels}$  and on the marsh surface  $V_{marsh}$ .

measured one. Moreover, the timescale of delay indicated from the distribution in Figure 8b ( $\sim 50$  min) well matches the results of the direct simulation with  $V_{channel} = 0.5$  m/s and  $V_{marsh} = 0.025$  m/s ( $\sim 50$  min; see Figure 5b).

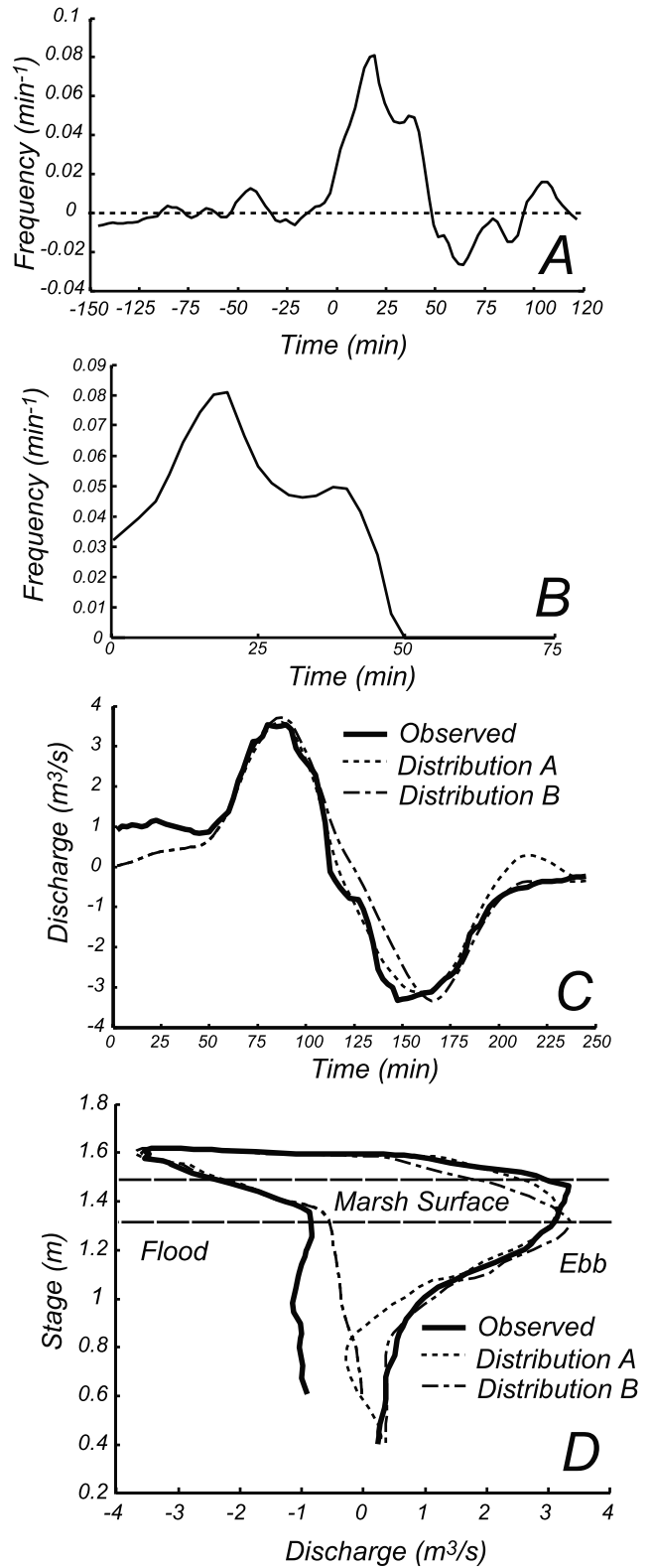


**Figure 8.** Determination of the distribution of travel time from measured discharges and the continuity model. (a) Deconvolution of the measured discharge from the continuity model. (b) Distribution of travel time calculated from the positive part in Figure 7a. Convolution of the continuity model with the distribution of travel time reported in Figures 8a and 8b: (c) time-discharge relationship and (d) stage-discharge relationship.

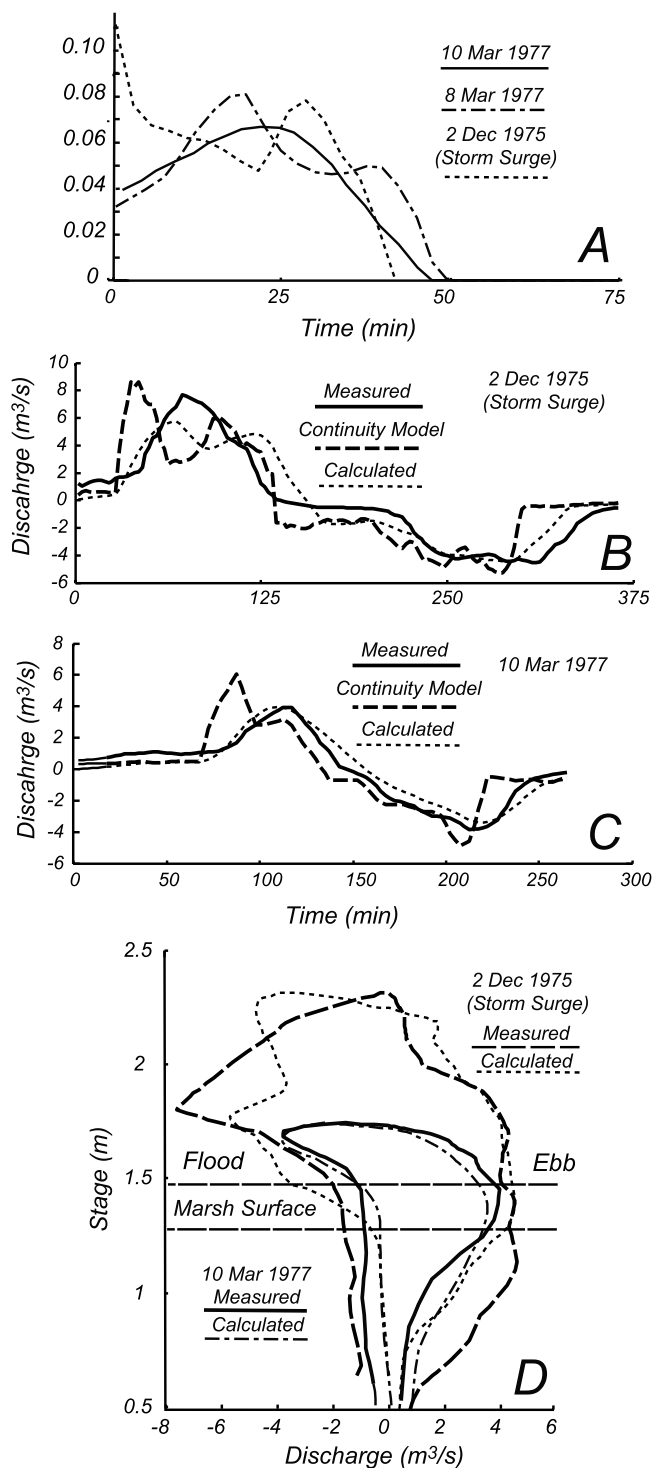


**Figure 9.** Determination of the distribution of travel time for the storm surge of 2 December 1975 and 8 March 1977. (a) Travel time calculated with a deconvolution of the measured discharge from the continuity model; comparison between measured discharge, discharge obtained from the continuity model, and the geomorphologic unit response model presented herein. (b) Storm surge of 2 December 1975. (c) Spring tide of 10 March 1977. (d) Measured and simulated stage-discharge relationship for the storm surge of 2 December 1975 and the spring tide of 8 March 1977.

[40] The same procedure was applied to the storm surge of 2 December 1975 and the spring tide of 8 March 1977 (Figure 9). All the travel time distributions extracted from these data exhibit a maximum travel time (also known as concentration time) around 50 min (Figure 9a) and well match the measured discharge (Figures 9b, 9c, and 9d).

## 5. Discussion and Conclusions

[41] The TIGER model presented herein and based on an extension of the continuity model of *Boon* [1975] allows linking the asymmetry in discharge peaks during overbank flow to the distribution of travel times of water particles within the salt marsh watershed. The importance of this result stems from its ability to relate the travel time distribution and the hydrodynamics of tidal watersheds to the geomorphic structure of the salt marsh and specifically to the distance traveled by water particles both within the channel network and on the marsh surface.

[42] The TIGER model presented herein addresses two important limitations of the *Boon* [1975] model indicated by *Healey et al.* [1981]. The velocity surges are delayed, thus producing realistic discharge peaks above and below the marsh platform during flood and ebb, respectively. The moving average embedded in the convolution integral of equation (3) smoothes the discharge oscillations that are characteristics of the continuity model of *Boon* [1975] and are produced by sudden changes in the rate of tidal oscillations. The model results are also in agreement with the field study of *French and Stoddart* [1992], which ascribes the existence of flow transients to the discontinuous prism-stage relationship, captured in our model by the hypsometric curve in equation (3). *French and Stoddart* [1992] also indicate that the asymmetry of creek velocity is due to differential flow resistance for channel and overbank flow, which is embedded in our framework in the different tidal velocities for the channels and the marsh surface.

[43] Recently, *Rinaldo et al.* [1999a] and *Marani et al.* [2003] presented a model that links the peak tidal discharge to the morphology of the tidal basin through the definition of appropriate watersheds for each tidal channel. The model accounts for the propagation of the wave in the channels but does not include the delay in tide propagation on flats and salt marshes, over which the flow is considerably slower because of bottom friction and vegetation. Moreover, in this modeling framework the continuity equation is not considered, limiting its applicability to peak flows rather than full tidal cycles.

[44] Our formulation paves the way for the application of recent results on the geomorphic structure of salt marshes and the scaling properties of tidal networks [*Fagherazzi et al.*, 1999; *Marani et al.*, 2003; *Novakowski et al.*, 2004; *Feola et al.*, 2005; *Hood*, 2007] to the study of marsh creek hydrology. For example, the distribution of travel distances on the marsh surface introduced by *Marani et al.* [2003] bears important consequences for the tidal velocity asymmetry during overbank flow, since it is directly linked to the travel time of water particles. Conversely, from measurements of tidal flow at a specific cross section we can infer important morphological information on the salt marsh structure, in a way that resembles the analysis by *Rinaldo et al.* [1995] for fluvial watersheds. Specifically, if we know the hypsometric curve of the marsh area relative to a

specific creek cross section, we can infer the distribution of travel times from measurements of tidal velocity at the outlet of the watershed. The distribution of travel times is critical for the determination of the residence time of water particles on the marsh platform, which in turn is linked to many biogeochemical processes like nutrients uptake and salt removal from the marsh soil.

[45] An important result is that the travel time distributions extracted from tidal cycles having a different excursion are similar (e.g., maximum residence time around 50 have min) even though the velocity of propagation of the tidal signal changes as a function of water depth. This is because the asymmetry in storm surges is dictated by the delay in signal propagation over the marsh surface when the platform is just flooded or almost drained, i.e., for small water depths rather than for high water levels (slack water). The system therefore responds in a similar way for tides of different amplitude since the critical instant determining the magnitude of the storm surge is when the flooding/drainage of the marsh platform occurs, rather than for high tide conditions.

[46] Our framework is valid only if the drainage area of each channel is constant during a tidal cycle. *Torres and Styles* [2007] showed that during high stages of the tidal cycle the hydrodynamics is only partly controlled by the creeks and that large-scale gradients in surface water in the intertidal area can give rise to flow exchanges between contiguous marsh creeks, producing flow reversals. Similar results are presented by *Temmerman et al.* [2005b], who show that during shallow inundation cycles almost all water is supplied via the creek system, while during higher inundation cycles the water is directly supplied via the marsh edge. Under these conditions the continuity model of *Boon* [1975] loses its applicability since the watershed area varies in time. However, this hydrodynamic behavior is limited to high tide stages when the water depth on the marsh platform is high enough to allow consistent water fluxes among different tidal channel watersheds. Velocity surges occur instead just after the flooding and the drainage of the marsh platform, when the hydrodynamics is still strongly controlled by the creeks and the watershed boundaries are fixed. The application of our model is then valid at the beginning of marsh flooding and at the end of marsh drainage, which are the most geomorphologically significant stages of the tidal cycle, as they are associated with the peak velocities. Caution should be used in the application of the model during high tide conditions.

[47] In this preliminary study we have considered a flat marsh platform and derived the drainage patterns following the gradients of water surface [see *Rinaldo et al.*, 1999b]. However, subtle differences in microtopography and the presence of channel levees can influence the water pathways during flooding and ebbing. A thorough analysis with high-resolution data is thus deemed necessary for future work.

[48] Finally, our modeling framework provides important results for marsh reconstruction and rehabilitation projects. For example, the presence of ditches on the marsh surface can reduce the average travel time of water particles, thus promoting a faster response of the system to tidal oscillations and higher peak discharges in the channels. The model can also estimate the residence time of the water on the

marsh surface, which regulates ecological functions critical for restoration projects.

[49] **Acknowledgments.** This research was supported by NSF through the VCR-LTER program award GA10618-127104, by the Office of Naval Research award N00014-07-1-0664, and by the Department of Energy NICCR program. We would like to thank Greg Pasternack, Ray Torres, and Marco Marani for their thoughtful revision of the manuscript.

## References

- Bayliss-Smith, T. P., R. Healey, R. Lailey, T. Spencer, and D. R. Stoddart (1978), Tidal flows in salt marsh creeks, *Estuarine Coastal Mar. Sci.*, *9*, 235–255.
- Boon, J. D. (1975), Tidal discharge asymmetry in a salt marsh drainage system, *Limnol. Oceanogr.*, *20*, 71–80.
- Carniello, L., A. Defina, S. Fagherazzi, and L. D'Alpaos (2005), A combined wind wave–tidal model for the Venice lagoon, Italy, *J. Geophys. Res.*, *110*, F04007, doi:10.1029/2004JF000232.
- Chow, V. T., D. R. Maidment, and L. W. Mays (1988), *Applied Hydrology*, McGraw-Hill, New York.
- Cox, D. R., and H. D. Miller (1965), *The Theory of Stochastic Processes*, Methuen, London.
- D'Alpaos, L., and A. Defina (2007), A mathematical modeling of tidal hydrodynamics in shallow lagoons: A review of open issues and applications to the Venice lagoon, *Comput. Geosci.*, *33*(4), 476–496.
- D'Odorico, P., and R. Rigon (2003), Hillslope and channel contributions to the hydrologic response, *Water Resour. Res.*, *39*(5), 1113, doi:10.1029/2002WR001708.
- Fagherazzi, S. (2002), Basic flow field in a tidal basin, *Geophys. Res. Lett.*, *29*(8), 1221, doi:10.1029/2001GL013787.
- Fagherazzi, S., A. Bortoluzzi, W. E. Dietrich, A. Adami, S. Lanzoni, M. Marani, and A. Rinaldo (1999), Tidal networks: 1. Automatic network extraction and preliminary scaling features from digital elevation maps, *Water Resour. Res.*, *35*(12), 3891–3904.
- Fagherazzi, S., P. L. Wiberg, and A. D. Howard (2003), Tidal flow field in a small basin, *J. Geophys. Res.*, *108*(C3), 3071, doi:10.1029/2002JC001340.
- Fagherazzi, S., M. Marani, and L. K. Blum (Eds.) (2004), *The Ecogeomorphology of Tidal Marshes*, *Coastal Estuarine Stud. Ser.*, vol. 59, edited by, 268 pp., AGU, Washington, D. C.
- Feola, A., E. Belluco, A. D'Alpaos, S. Lanzoni, M. Marani, and A. Rinaldo (2005), A geomorphic study of lagoonal landforms, *Water Resour. Res.*, *41*, W06019, doi:10.1029/2004WR003811.
- French, J. R., and D. R. Stoddart (1992), Hydrodynamics of salt-marsh creek systems: Implications for marsh morphological development and material exchange, *Earth Surf. Processes Landforms*, *17*(3), 235–252.
- Gupta, V. K., E. Waymire, and C. T. Wang (1980), A representation of an instantaneous unit hydrograph, *Water Resour. Res.*, *16*, 855–862.
- Healey, R. G., K. Pye, D. R. Stoddart, and T. P. Bayliss-Smith (1981), Velocity variations in salt marsh creeks, Norfolk, England, *Estuarine Coastal Shelf Sci.*, *13*, 535–555.
- Hood, W. G. (2007), Scaling tidal channel geometry with marsh island area: A tool for habitat restoration, linked to channel formation process, *Water Resour. Res.*, *43*, W03409, doi:10.1029/2006WR005083.
- Kirkby, M. (1986), A runoff simulation model based on hillslope topography, in *Scale Problems in Hydrology*, edited by V. K. Gupta et al., pp. 39–56, D. Reidel, Dordrecht, Netherlands.
- Lawrence, D. S. L., J. R. L. Allen, and G. M. Havelock (2004), Salt marsh morphodynamics: An investigation of tidal flows and marsh channel equilibrium, *J. Coastal Res.*, *20*(1), 301–316.
- Marani, M., E. Belluco, A. D'Alpaos, A. Defina, S. Lanzoni, and A. Rinaldo (2003), On the drainage density of tidal networks, *Water Resour. Res.*, *39*(2), 1040, doi:10.1029/2001WR001051.
- Mesa, O. J., and E. R. Mifflin (1986), On the relative role of hillslope and network geometry in hydrologic response, in *Scale Problems in Hydrology*, edited by V. K. Gupta et al., pp. 181–190, D. Reidel, Dordrecht, Netherlands.
- Myrick, R. M., and L. B. Leopold (1963), Hydraulic geometry of a small tidal estuary, *U.S. Geol. Surv. Prof. Pap.*, *422-B*, 18 pp.
- Novakowski, K. I., R. Torres, L. R. Gardner, and G. Voulgaris (2004), Geomorphic analysis of tidal creek networks, *Water Resour. Res.*, *40*, W05401, doi:10.1029/2003WR002722.
- Pethick, J. S. (1972), Salt marsh morphology, Ph.D. dissertation, Univ. of Cambridge, Cambridge, U. K.

- Pethick, J. S. (1980), Velocities, surges and asymmetry in tidal channels, *Estuarine Coastal Mar. Sci.*, *11*, 331–345.
- Rinaldo, A., A. Marani, and R. Rigon (1991), Geomorphological dispersion, *Water Resour. Res.*, *28*(4), 513–525.
- Rinaldo, A., G. K. Vogel, R. Rigon, and I. Rodriguez-Iturbe (1995), Can one gauge the shape of a basin?, *Water Resour. Res.*, *31*, 1119–1128.
- Rinaldo, A., S. Fagherazzi, S. Lanzoni, M. Marani, and W. E. Dietrich (1999a), Tidal networks: 3. Landscape-forming discharges and studies in empirical geomorphic relationships, *Water Resour. Res.*, *35*(12), 3919–3929.
- Rinaldo, A., S. Fagherazzi, S. Lanzoni, M. Marani, and W. E. Dietrich (1999b), Tidal networks: 2. Watershed delineation and comparative network morphology, *Water Resour. Res.*, *35*(12), 3905–3917.
- Rodriguez-Iturbe, I., and J. B. Valdes (1979), The geomorphologic structure of hydrologic response, *Water Resour. Res.*, *15*(6), 1409–1420.
- Rodriguez-Iturbe, I., and A. Rinaldo (1997), *Fractal River Basins: Chance or Self-Organization*, Cambridge Univ. Press, Cambridge, U. K.
- Sherman, L. K. (1932), Streamflow from rainfall by the unit-graph method, *Eng. News Rec.*, *108*, 501–505.
- Shreve, R. L. (1969), Stream lengths and basin areas in topologically random channel networks, *J. Geol.*, *77*, 397–414.
- Temmerman, S., T. J. Bouma, G. Govers, Z. B. Wang, M. B. De Vries, and P. M. J. Herman (2005a), Impact of vegetation on flow routing and sedimentation patterns: Three-dimensional modeling for a tidal marsh, *J. Geophys. Res.*, *110*, F04019, doi:10.1029/2005JF000301.
- Temmerman, S., T. J. Bouma, G. Govers, and D. Lauwaet (2005b), Flow paths of water and sediment in a tidal marsh: Relations with marsh developmental stage and tidal inundation height, *Estuaries*, *28*(3), 338–352.
- Torres, R., and R. Styles (2007), Effects of topographic structure on salt marsh currents, *J. Geophys. Res.*, *112*, F02023, doi:10.1029/2006JF000508.
- van der Tak, L. D., and R. L. Bras (1990), Incorporating hillslope effects into the geomorphological instantaneous unit hydrograph, *Water Resour. Res.*, *26*(10), 2393–2400.
- Woldenburg, M. J. (1972), Relations between Horton's laws and hydraulic geometry as applied to tidal networks, *Harvard Pap. Theoret. Geogr.*, *45*, 1–39.
- Zeff, M. L. (1999), Salt marsh tidal channel morphometry: Applications for wetland creation and restoration, *Restor. Ecol.*, *7*, 205–211.

---

S. Fagherazzi, Department of Earth Sciences and Center for Computational Science, Boston University, Boston, MA 02122, USA. (sergio@bu.edu)

M. Hannion, Department of Geological Sciences, Florida State University, Tallahassee, FL 32306, USA.

P. D'Odorico, Department of Environmental Sciences, University of Virginia, Charlottesville, VA 22904, USA.